

Experimental study of the transport of mixed sand and gravel

Peter R. Wilcock, Stephen T. Kenworthy, and Joanna C. Crowe

Department of Geography and Environmental Engineering, Johns Hopkins University
Baltimore, Maryland, USA

Abstract. We measured a wide range of transport rates for five different sand/gravel mixtures in a laboratory flume. Each mixture used the same gravel, and sand was added to produce mixtures containing 6, 15, 21, 27, and 34% sand. Control of other variables allows us to isolate the effect of bed sand content on transport. As sand content increases, gravel transport rates increase by orders of magnitude, even though the proportion of gravel in the bed decreases. The increase in gravel transport rate is most rapid over the range of bed sand content between 15 and 27%. The increase in transport rate is larger than predicted using standard scaling relations between transport rate and grain size, indicating that models of transport and sorting and predictions of stream channel response to sand inputs need to be revised to account for the influence of sand content. Bed surface grain size was measured at the end of each run. Surface grain size varied with sand content but showed little or no coarsening with flow strength and transport rate. This casts doubt on the idea that armor layers form at small flows and weaken or vanish with increasing flow and transport rate.

1. Introduction

A variety of natural or human actions, such as fire, logging, flow diversion, road construction, and urban or agricultural development can increase the supply of sand to a gravel bed river. An understanding of the river channel's response to sand inputs, as well as the fate of the sand, requires an understanding of the effect of sand content on transport rate. Previous work [Jackson and Beschta, 1984; Ikeda and Iseya, 1988; Wilcock, 1998] provides some indication that increased sand content can augment gravel transport rates beyond that which can be adequately accounted for in standard transport models. The purpose of the experiments described in this paper is to document the effect of river bed sand content on the transport rates of sand and gravel.

We measured flow and transport in four series of flume runs using a gravel sediment to which sand was added to produce mixtures containing 6, 15, 21, and 27% sand. The gravel and sand component of each mixture was identical: The gravel ranged in size from 2 to 64 mm with median 13 mm, and the sand size range was 0.5 to 2.0 mm with median 1 mm. For each of the four sediments, 9 or 10 flume runs were conducted over a range of water discharge. Each run was continued until the flow and transport reached a steady state, at which point flow rate, depth, and slope were measured along with transport rates of different size fractions. Combined with the results of earlier experiments conducted with the same gravel mixed with 34% sand in the 0.21–2.0 mm range [Wilcock and McArdell, 1993], the experimental results discussed here provide a direct evaluation of the effect of sand content on transport over a range of transport rates and for a range of sand content that encompasses much of the variation observed in natural streams.

In addition to measuring transport rate, we also measured the size distribution of the bed surface at the end of each run,

giving coupled observations of transport rate, bed surface composition, and flow. This is the information needed to develop an empirical model of transport rate referenced to the grains immediately available for transport on the bed surface. As discussed in detail elsewhere [e.g., Parker, 1990; Wilcock and McArdell, 1993; Wilcock, 2001], a general model for mixed-size sediment transport must be referenced to the bed surface composition in order to predict size sorting and transient adjustments of the flow/bed/transport system. The data presented here are the first comprehensive collection of coupled observations of transport rate, surface composition, and flow for a range of sediments. Previous field investigations have generally been limited to a single observation of bed surface composition at low flow; the bed composition associated with active transport is generally unknown. Some previous laboratory transport studies have included measurements of the bed surface composition, although the samples were collected using adhesives, which introduces uncertainty about the inclusion of subsurface sediment in the sample and which requires a conversion to allow comparison with transport and subsurface samples. We measure the surface with a simple point count method that permits direct comparison with volume-by-weight samples of the transport [Church *et al.*, 1987]. That the surface-based transport observations are made for a series of sediments defined by a controlled variation in sand content is an added benefit. Because surface-based transport observations require special effort and are relatively rare, the data discussed here are available as an AGU electronic supplement.¹

2. Previous Experiments

Previous experiments shed light on how gravel transport rates respond to a change in sand supply. Jackson and Beschta [1984] deposited a sandy gravel bed in a flume and, in a series

¹Supporting tables are available via Web browser or via Anonymous FTP from <ftp://agu.org>, directory "apend" (Username = "anonymous", Password = "guest"); subdirectories in the ftp site are arranged by paper number. Information on searching and submitting electronic supplements is found at http://www.agu.org/pubs/esupp_about.html.

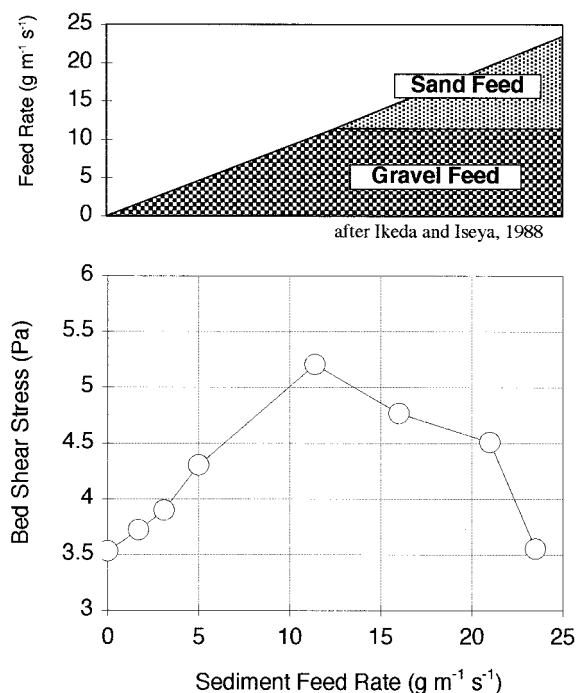


Figure 1. Results of experiments by *Ikeda and Iseya* [1988]. As sand is added to gravel feed, the stress needed to transport the sediment decreases even though the rate of transport is larger.

of eight runs, allowed the deposit to armor by running clear water over the bed until no further sediment emerged from the flume. Sand was then added to the clear water inflow, and additional gravel was transported out of the channel, demonstrating that additional sand was able to induce entrainment and transport from an armored gravel bed.

The clearest demonstration of the effect of sand on gravel transport has been achieved with eight runs in a small flume (10 cm wide) by *Ikeda and Iseya* [1988]. In the first five runs they fed fine gravel (2.7 mm) at a rate that increased from run to run. The discharge was held constant, and the depth varied little, so as the feed rate increased, the bed slope increased to produce a larger bed shear stress to carry the larger transport rate (Figure 1). For the last three runs the rate of gravel input was held constant, and well-sorted medium sand (0.35 mm) was also fed into the flume, thereby increasing the total feed rate. The bed slope decreased, indicating that a smaller shear stress was needed to transport the sand-gravel mixture, even though the transport rate of the gravel remained unchanged and the total transport rate increased. This demonstrates that the same amount of gravel could be transported at the same flow, even though additional sand is added to the system. In fact, the decrease in shear stress indicates that more gravel could be carried with the same shear stress if sand is added to the system.

Although indicative, there are several aspects of the *Ikeda and Iseya* experiments that limit direct extrapolation to the field case. The sediment used (0.37 and 2.6 mm) was much smaller than typical sediment in a gravel bed river, particularly in the gravel fraction, and the difference in size between the sand and gravel fractions was also very small. The sediment size distribution was also strongly bimodal with no overlap between the modes, whereas even strongly bimodal sediments

in the field typically contain intermodal sediment. The Froude numbers in the experiments were much larger than typically found under conditions of alluvial transport, and the very shallow (≈ 1 cm) flow depth limited the accuracy of depth measurements. Despite these problems the experiments of *Ikeda and Iseya* show unequivocally that gravel transport rates can be maintained or even augmented in the presence of additional sand.

The experiments presented here build on this previous work in several ways. First, the size range of the experimental sediment (0.5–64 mm) is unusually large for a flume study and is directly representative of many gravel bed rivers. Second, a wide range of transport rates was measured for each sediment, allowing us to examine the influence of sand content on not just a single transport rate but on the trend between transport rate and flow strength. Third, the bed surface grain-size distribution was measured at the end of each run, providing a measure of the bed response to varying flow and sand content. Finally, sediment was recirculated in the present experiments, providing a direct comparison between the composition of the bed and the resulting transport.

3. Methods

3.1. Sediment

The experimental sediments were prepared by adding different amounts of sand to a gravel mixture (Table 1 and Figure 2). The gravel ranged in size from 2.0 to 64 mm and is identical to the gravel portion of the bed of many colors (BOMC) sediment previously reported on by *Wilcock and McArdell* [1993, 1997]. In four of the sediments the sand varied in size between 0.5 and 2.0 mm. Approximately one half of the sand in the fifth sediment (BOMC) was in the range of 0.21–0.5 mm, making the sand size approximately half that of the other four (Table 1). The proportion of sand in the mixtures varied from 6.2 to 34.3%; the four new sediments were named according to the target sand content such that the sediment name and actual sand content were J06 (6.2%), J14 (14.9%), J21 (20.6%), and J27 (27%). Standard $1/2\phi$ size fractions were used to define all fractions coarser than 1.0 mm; grains in the 0.5–1.0 mm range were combined into one fraction.

The mean specific gravity of all size fractions was 2.61; the maximum deviation from this mean was 5%. The 4.0–8.0 mm size fractions contain some chalky limestone clasts, which lowers the mean density for these fractions to 2.49. The clasts between 8.0 and 32 mm contain a larger proportion of magic

Table 1. Grain-Size Statistics

	Mean, mm	Standard Deviation ϕ	Median D_{50} , mm	D_{90} , mm
Gravel	12.2	1.28	13.4	39
Sand	1.0	0.53	1.0	1.7
Sand (BOMC) ^a	0.5	0.82	0.5	1.35
J06	10.5	1.54	12.2	38
J14	8.4	1.77	9.8	37
J21	7.3	1.88	8.4	36
J27	6.1	1.96	6.7	33
BOMC	4.1	2.41	5.3	31

^aBOMC, bed of many colors.

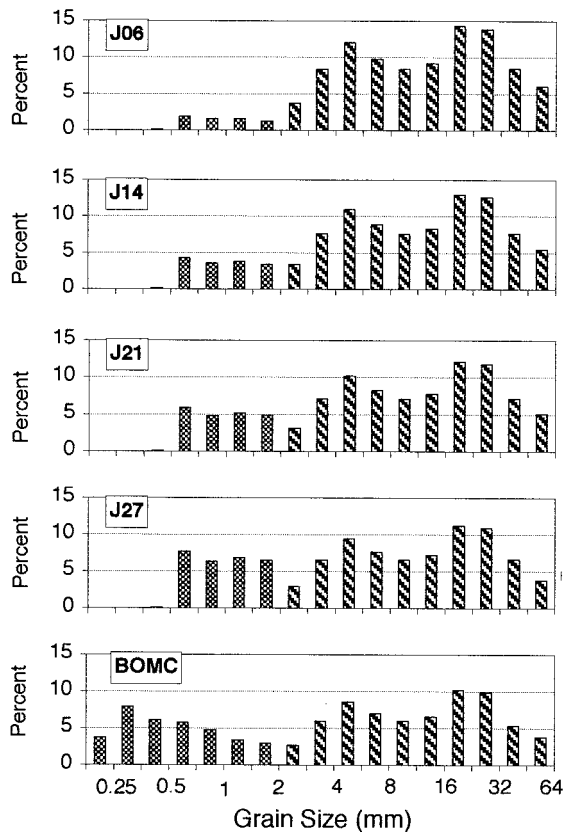


Figure 2. Grain-size distribution of the experimental sediments.

minerals and have a mean specific gravity in the range 2.69–2.73.

3.2. Transport and Hydraulic Measurements

We conducted 38 experimental runs with the four new mixtures. Combined with 10 BOMC runs, the 48 experimental runs reported here span a threefold range in water discharge and a 7 order-of-magnitude range in transport rate. The mean hydraulic and transport observations for each run are given in Table 2. The complete size distributions of the bed surface and transport are available in the AGU electronic supplement.

The experiments were conducted in a tilting laboratory flume with clear sidewalls. The channel is 60 cm wide with a working length of 790 cm. A 120 cm artificially roughened bed was placed at the upstream of the working section to develop the boundary layer before the flow encounters the loose sediment bed. Downstream of the working section is a 120 cm long, full-width sediment trap. Water and sediment were recirculated separately. Water temperature was typically between 19°C and 23°C. Most of the water passed with no overflow over the sediment trap and into a tailbox and then through two or three centrifugal pumps and a 20 cm pipe to the upstream end of the flume. A small portion of the water discharge and the sediment finer than 16 mm passed through the sediment trap and was recirculated with an air-driven diaphragm pump through a 5 cm plastic hose to the flume head box. Coarser grains were caught on a 16 mm screen inside the sediment trap and manually returned to the flume head box at periods ranging from 1 to 5 min, depending on transport rate.

Sediment transport was sampled with three different meth-

ods, a result of the separate recirculation paths of the fine and coarse grains and the competing requirements that we minimize disturbance of the transport during a run while also collecting enough samples to adequately measure the transport rates. Grains finer than 16 mm were sampled by diverting the sediment recirculation line to an open hose and directing the discharge onto a 0.21 mm sieve placed inside a 100 L funnel. All of the sediment was retained on the sieve, while the water was immediately returned to the sediment recirculation system through a hose at the base of the funnel. This system allowed the transport to be sampled over a wide range of periods, depending on the transport rate.

Because total transport rate varies over a much wider range than the transport size distribution, the sampling period necessary to obtain a reliable estimate of the total transport rate is much longer than that needed to determine the transport size distribution. During most of a transport sample period, only the total volume of transported sediment was measured, and the sample was then returned to the recirculation line through the sampling funnel within a period of 30–60 s. This procedure permits measurement of the total transport rate with negligible disruption of the recirculating transport system. Samples for size analysis were collected at the end of a run to determine the grain size of the transport and the conversion from volumetric to mass transport rate. These samples were returned to the flume prior to the next run. Fractional transport rates are calculated as $q_{bi} = (p_i)q_b$, where p_i is the proportion of each fraction in transport and q_b is the total transport rate.

The coarser sediment caught on the screen in the sediment trap was recirculated by hand and was sampled nearly continuously. The gravel fractions were separated by size, and the mass of each coarse fraction was typically determined with a hanging balance. On some occasions the number of grains of each size were counted, and a calibrated number-to-mass conversion was used to determine transport rate. An advantage of manual recirculation is that we could monitor the rare motion of the coarsest grains throughout the run, providing a long time series and a more reliable estimate of their transport rate.

The elevation of the water and bed surfaces during a run were measured with point gages and referenced to the horizontal plane of a still water surface. Discharge was measured with a Venturi meter in the water return pipe. Water discharge in the sediment recirculation line took one of two nearly constant values, depending on whether the sediment pump was driven by compressed air from the building supply or from a portable air compressor used to increase sediment recirculation capacity at high transport rates. In both cases the sediment recirculation discharge was a small fraction of the main water discharge. Mean flow velocity was determined from the discharge, the mean flow depth, and flume width. Surface velocity was measured by timing the travel of surface tracers over a 5 m distance. Plastic bottle caps each with a thickness of 1.5 cm and a diameter of 3 cm were used as tracers because they were found to float fully submerged with the upper side just at the water surface. The mean of the five fastest times out of 10 observations was used to determine the surface velocity. Tracer tracks within 10 cm of the wall were discarded. Following the first seven runs of the J06 series, it was found that the manometer used to determine the pressure drop on the Venturi meter was not properly bled and that the calculated discharge was apparently too small. For these runs we estimate the mean flow velocity based on a regression between mean velocity and surface velocity, which showed a tight correlation for all subse-

Table 2. Mean Flow and Transport Observations

Run	Unit Discharge, $\text{m}^2 \text{s}^{-1}$	Flow Depth, m	Water Slope	Bed Shear Stress, Pa	Gravel Transport, $\text{g m}^{-1} \text{s}^{-1}$	Sand Transport, $\text{g m}^{-1} \text{s}^{-1}$
J06-1	0.0781	0.104	0.0044	4.10	2.09E - 04 ^a	1.33E - 05
J06-2	0.0862	0.108	0.0049	4.90	2.52E - 03	6.17E - 06
J06-3	0.0959	0.104	0.0094	8.70	9.23E - 02	2.36E - 04
J06-4	0.1032	0.102	0.0133	11.3	1.40E + 00	2.90E - 03
J06-5	0.0906	0.103	0.0067	6.18	2.01E - 02	4.44E - 05
J06-6	0.1048	0.103	0.0092	8.29	4.29E - 01	7.98E - 04
J06-7	0.1212	0.106	0.0158	16.0	1.45E + 01	3.17E - 02
J06-8	0.0778	0.105	0.0056	5.42	3.29E - 03	3.26E - 05
J06-9	0.1282	0.109	0.0176	17.5	2.95E + 01	6.21E - 02
J06-10	0.1334	0.108	0.0204	23.6	2.04E + 02	1.57E - 01
J14-1	0.1259	0.117	0.0165	16.5	5.08E + 01	5.51E - 01
J14-2	0.1243	0.109	0.0173	19.1	7.29E + 01	1.56E + 00
J14-3	0.0838	0.107	0.0061	6.43	2.91E - 02	7.32E - 04
J14-4	0.1013	0.104	0.0106	9.74	1.70E + 00	8.13E - 02
J14-5	0.1103	0.106	0.0144	16.1	1.19E + 01	5.96E - 01
J14-6	0.0788	0.102	0.0044	4.38	1.81E - 02	1.03E - 03
J14-7	0.0957	0.106	0.0083	8.63	1.48E + 00	6.31E - 02
J14-8	0.0909	0.106	0.0076	7.27	5.08E - 01	3.84E - 02
J14-9	0.1334	0.117	0.0157	20.1	1.14E + 02	1.90E + 00
J21-1	0.1259	0.118	0.0155	15.9	1.25E + 02	9.41E + 00
J21-2	0.0785	0.108	0.0043	4.07	4.21E - 01	6.53E - 02
J21-3	0.0888	0.102	0.0071	6.64	5.32E + 00	8.04E - 01
J21-4	0.0992	0.105	0.0114	10.8	9.92E + 00	2.01E + 00
J21-5	0.0734	0.109	0.0034	3.35	9.81E - 02	3.50E - 02
J21-6	0.0903	0.104	0.0078	7.21	1.04E + 01	2.43E + 00
J21-7	0.0654	0.099	0.0032	2.82	1.30E - 02	3.67E - 03
J21-8	0.1119	0.102	0.0171	16.1	1.36E + 02	1.61E + 01
J21-9	0.1203	0.107	0.0175	18.6	NA ^b	NA ^b
J27-1	0.0651	0.102	0.0029	2.78	2.39E - 01	2.44E - 01
J27-2	0.0892	0.101	0.0070	6.91	2.26E + 01	1.40E + 01
J27-3	0.0495	0.110	0.0010	1.10	7.57E - 04	2.17E - 03
J27-4	0.0572	0.101	0.0026	2.50	7.74E - 02	1.28E - 01
J27-5	0.0816	0.093	0.0074	6.57	2.09E + 01	6.79E + 00
J27-6	0.0749	0.098	0.0043	3.96	3.44E + 00	2.18E + 00
J27-7	0.1029	0.106	0.0080	7.91	4.68E + 01	2.00E + 01
J27-8	0.1128	0.106	0.0098	9.46	6.78E + 01	3.73E + 01
J27-9	0.1255	0.106	0.0143	11.5	2.37E + 02	1.02E + 02
J27-10	0.1297	0.111	0.0168	17.4	5.27E + 02	2.51E + 02
BOMC 14c	0.0285	0.111	0.00059	0.57	3.92E - 05	2.27E - 03
BOMC 7a	0.0342	0.110	0.00088	0.85	1.00E - 20	3.29E - 02
BOMC 14b	0.0362	0.109	0.00091	0.86	1.16E - 04	3.85E - 02
BOMC 7b	0.0397	0.111	0.0011	1.07	1.81E - 04	9.50E - 02
BOMC 7c	0.0480	0.105	0.0017	1.60	2.73E - 03	4.24E - 01
BOMC 1	0.0672	0.120	0.0018	1.83	7.62E - 02	5.72E + 00
BOMC 2	0.0667	0.112	0.0032	3.14	4.40E - 01	6.66E + 00
BOMC 6	0.0786	0.096	0.0069	5.94	3.51E + 01	8.99E + 01
BOMC 4	0.0812	0.094	0.0077	6.47	4.42E + 01	1.13E + 02
BOMC 5	0.0950	0.088	0.0162	13.1	3.05E + 02	2.67E + 02

^aRead, for example, 2.09E - 04 as 2.09×10^{-4} .

^bNA is not available.

quent runs. For these seven runs the reported velocity and discharge per unit width are 10–15% larger than that calculated from the Venturi measurements, and the reported bed shear stress is 0–3% smaller.

The bed shear stress was corrected for sidewall effects, following the method of *Vanoni and Brooks* [1957], as modified by *Chiew and Parker* [1994]. The resulting shear stress was consistently 8% smaller than that calculated using the flow depth and was 24% larger than that calculated using the flow hydraulic radius. Because the sediment bed was essentially planar in almost all runs, no further adjustments were made to estimate the mean bed stress. Long, low dunes, with an irregular slip

face and dune height smaller than 1 cm were present in the two BOMC runs with largest flow strength, such that the estimated shear stress in these runs includes some form drag, although we estimate it to be a small proportion of the total bed stress.

3.3. Bed Surface Grain-Size Distribution

All grains of each size fraction had been previously painted a different color [*Wilcock and McArdeil*, 1993]. This unusual step allows us to measure the grain-size distribution of the bed surface using point counts on photographs of the bed, which provides a reliable and statistically tractable estimate of the bed surface grain-size distribution. The grain-size distribution

of the bed surface was measured by projecting photographs of the bed onto a grid and tallying the grain color (hence size) falling on the grid intersections. Each photograph covered a bed section with dimensions of 20 cm in the cross-stream direction and 28 cm in the downstream direction. Individual grains were visible for all fractions. Two adjacent photographs provided continuous cross-stream coverage of 40 cm. The remaining 10 cm on each side of the flume was not photographed. Point counts were conducted for the downstream 4 m of the test section, and an individual surface size sample typically used 3920 points, although occasionally the number of points counted was smaller by a few percent because the film exposure did not permit reliable counts in small areas of the bed. A large number of points was used in order to estimate the proportion F_i of each size fraction on the bed surface. The grid-by-number method used here to determine the bed surface grain-size distribution has been shown to be equivalent to the volume-by-weight method commonly used in bulk sampling and sieve analyses [Kellerhals and Bray, 1971; Church *et al.*, 1987]. On the basis of previous analysis of replicate point counts and a comparison between bulk and screeded beds we suggest that a conservative estimate of the error in measuring F_i is $\pm 30\%$ (e.g., for an observed $F_i = 0.1$ the true value is likely to fall within 0.07 and 0.13). The actual error in most cases should be considerably smaller [Wilcock and McArdell, 1993].

3.4. Experimental Procedure

The sediment bed was thoroughly mixed by hand and screeded flat; the bed was always prepared by the same person in order to make the initial bed as consistent as possible. Repeated point counts of the initial screeded beds demonstrated the consistency of the initial bed surface grain-size distribution. To save time, the sediment bed was not remixed and screeded before each run but 3 or 4 times over the entire series of runs with each sediment. Within a sequence of runs following remixing and screeding, flume runs were always conducted with a large increase in transport rate from the preceding run. Because the sediment mobilized in any run was completely incorporated into the much larger amount of sediment mobilized in subsequent runs in the same sequence, the bed surface observed at the end of each run could be attributed to the initial prepared bed and not, for example, to a sorted surface left by a larger transport rate [Parker and Wilcock, 1993].

A suite of hydraulic and transport measurements were made during each run, including water discharge, surface velocity, water and bed surface elevations, volumetric sampling of the finer-grained transport, and mass sampling of the coarser-grained transport. At the end of the run, samples of the finer-grained transport were saved for size analysis. Steady state conditions appropriate for transport sampling were defined by a stable mean in transport rate and size distribution. These final samples can be correlated with the bed surface at the end of the run. The flume was then drained, and the bed surface was photographed. After the transport samples had been sieved and returned to the upstream end of the flume, the flume was filled, and another run in the sequence was begun at a larger transport rate. After the last run in a series was completed, the bed was completely rehomogenized in preparation for the next series of runs.

4. Results

4.1. Bed Surface Grain-Size Distribution

The proportion of sand F_s on the bed surface at the end of runs is plotted in Figure 3a along with mean F_s of the initial beds ("Initial Bed Surface") and the sand content f_s in the bulk mixture ("Bulk"). In general, F_s is relatively insensitive to discharge but varies systematically with f_s . For J06 and J14, F_s is very small, indicating that most of the sand initially on the bed surface was progressively stored within the pores of the gravel mixture. Transport also reduced F_s for J21 and J27, although the decrease from its initial value is proportionately smaller and the presence of measurable sand on the bed surface suggests that the available sand storage within the bed has been filled. For BOMC, mean F_s is 47.5%, which is comparable to that of the initial bed surface (Figure 3a). Sand content increases with flow strength for BOMC, which Wilcock and McArdell [1993] attributed to the associated increase in the bed thickness actively involved in the transport. Larger flows are able to "mine" sand from deeper in the bed. Because of the large sand content of BOMC, only a portion of the exhumed sand is able to return to the bed subsurface.

Similar to F_s , median size (D_{50}) of the bed surface clearly varies with f_s and is less sensitive to discharge (Figure 3b). The change in surface D_{50} can be attributed in part to variation in sand content and in part to variation in the median size of the surface gravel D_g (Figure 3c). Note that the grain-size scale on Figures 3b and 3c is arithmetic, which tends to accentuate minor changes in grain size, particularly at larger sizes. There is some indication that D_g increases with discharge, although the trend is weak and noisy. In runs with BOMC we observed that the bed was typically in a state of partial transport [Wilcock and McArdell, 1993, 1997], meaning that a portion of the grains on the bed surface remained immobile throughout the run. The range of sizes in a state of partial transport increased consistently with flow strength, and full mobilization of all grains on the bed surface (with the exception of a small portion of the grains in the coarsest fraction) was achieved only at the largest flow [Wilcock and McArdell, 1997]. We did not make partial transport observations for the four new sediments, although we expect that a similar trend in partial transport occurred over the range of flow used for each sediment. Coarsening of the bed surface in a sediment recirculating flume is predominantly through kinematic sorting [Wilcock, 2001], by which finer grains are able to occupy space vacated by the entrainment of large grains, but not vice versa, leading to a downward movement of fine gains relative to coarse grains. Because coarse grain entrainment is necessary for kinematic sorting to operate, an increase in surface D_g with flow strength may be attributed to a corresponding increase in the proportion of coarse grains entrained during a run. We expect, but cannot explicitly demonstrate, that D_g would change little with increases in flow strength beyond that required to mobilize the entire bed surface.

The observation of little or no coarsening with increasing flow strength and transport rate has important implications for our understanding of streambed armor. A paradigm has developed that coarse armor layers evident at low flow tend to "break up" and become finer-grained as transport rate increases [e.g., Parker and Klingeman, 1982; Dietrich *et al.*, 1989]. This interpretation is based primarily on flume experiments in which sediment of a constant size is fed into the flume. Under these conditions, differences in grain mobility (which tend to

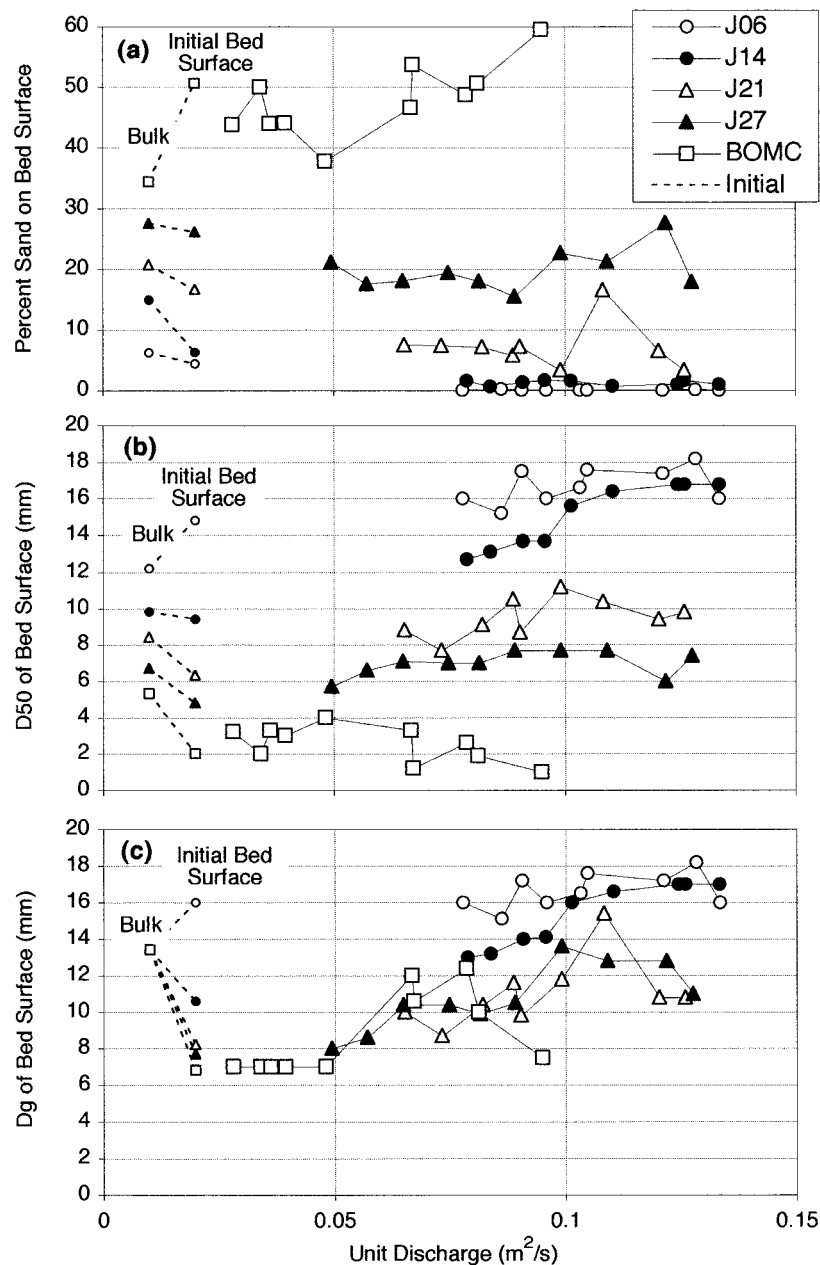


Figure 3. Grain-size distribution of the bed surface at the end of each run. (a) Percent sand on the bed surface. (b) Median grain size of the bed surface. (c) Median grain size of the gravel on the bed surface (size distribution truncated at 2 mm). Values corresponding to the bulk sediment and to the initial screeded bed surface are shown on the left side of each panel.

vary with both grain size and flow strength) may be expected to cause the surface to coarsen at smaller transport rates and to become finer at larger transport rates [Parker and Klingeman, 1982]. Our results in a recirculating flume indicate that the surface layer does not disappear as transport increases and may actually become slightly coarser over the range of partial transport. Inasmuch as the boundary conditions for natural streams fall somewhere between the two end-member cases represented by sediment feed and recirculating flumes, the idea that armor layers vanish with increasing transport rates does not appear to be general. Indeed, because the grain size of the transport in natural streams tends to increase with flow strength and transport rate, a property replicated by recircu-

lating flumes but not feed flumes, it appears likely that armor evolution with transport rate is much more subtle than previously thought and may be negligible [Wilcock, 2001].

4.2. Gravel Transport Rates as a Function of Sand Content

The primary objective of the experiments was to demonstrate the effect of sand content on transport rate. The variables that can be specified in a sediment recirculating flume are the sediment placed in the bed, the mean flow depth, and the water discharge [Parker and Wilcock, 1993]. Only sand content varied from mixture to mixture. Variations in mean flow depth were relatively minor, and discharge was varied from run to

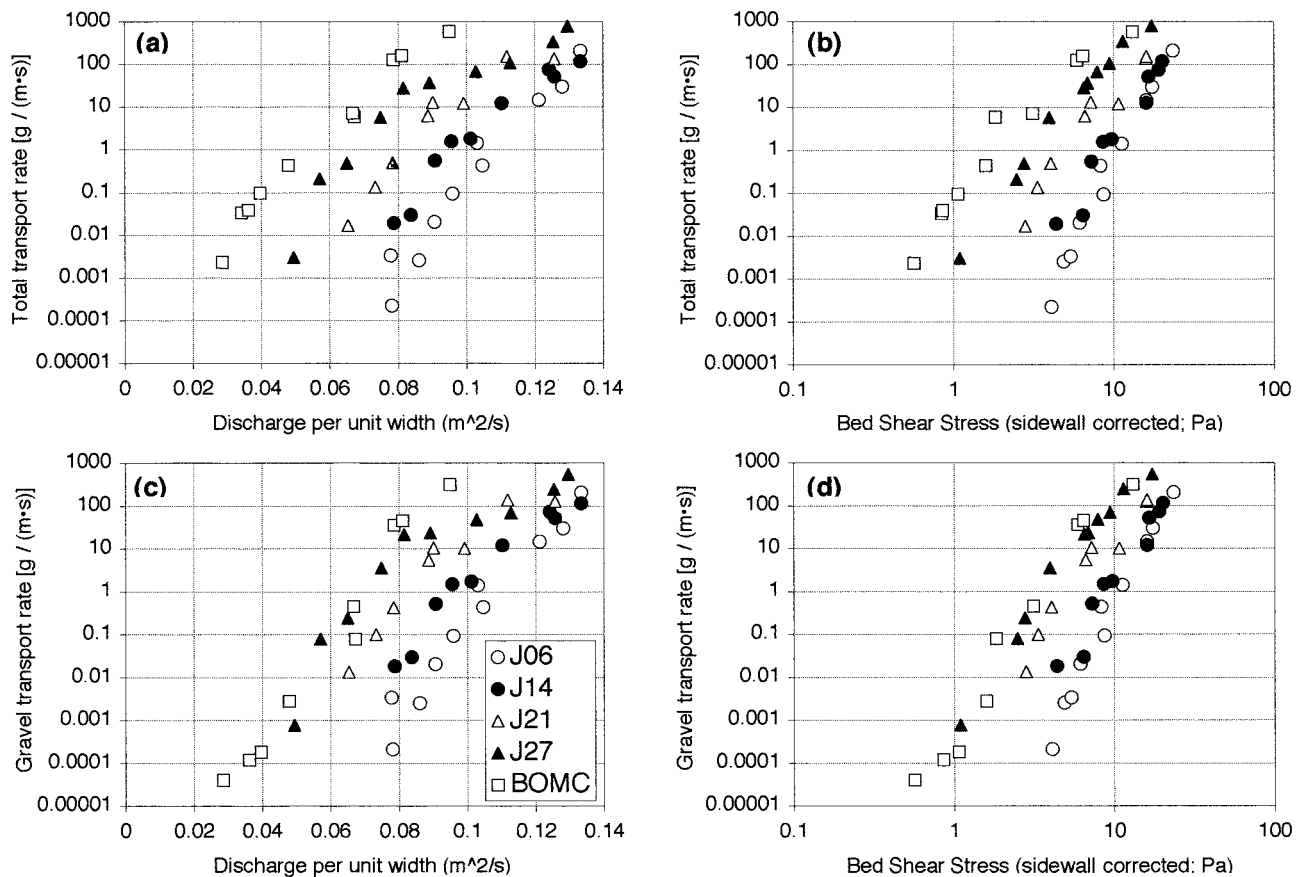


Figure 4. Transport rates for all experimental runs. (a) Total transport rate as a function of water discharge. (b) Total transport rate as a function of bed shear stress. (c) Gravel (>2 mm) transport rate as a function of water discharge. (d) Gravel (>2 mm) transport rate as a function of bed shear stress. Note that gravel transport rates are not scaled by the proportion of gravel in the bed.

run to produce different transport rates. As discharge increases, bed and water slope at equilibrium transport also increase. In our experiments the slope remained small (maximum 0.0204), and variations in slope from run to run may be expected to have essentially no direct effect on the transport [Fernandez-Luque and van Beek, 1976]. With small slopes and minor variation in flow depth a plot of transport rate versus discharge provides a simple and direct demonstration of the effect of sand content on transport rate. This effect is very large, with more than a 5 order-of-magnitude increase in transport rate from J06 to (BOMC) at some values of q (Figure 4a). Part of this increase represents rapid transport of the extra sand added to the mixtures. Of more particular interest is the effect of f_s on the transport rate of the gravel q_g . Again, the increase in transport rate with increasing f_s is very large (Figure 4c). Trends for the sandier mixtures (J21, J27, and BOMC) fall progressively above those for the less sandy mixtures (J06 and J14), and the spread in transport rate is as much as 5 orders of magnitude at some q .

The increase in q_g is all the more striking because q_g in Figure 4c is not scaled by the proportion of gravel in the bed. As f_s increases, the proportion of gravel in the mixture decreases proportionately. If sand content had no effect on gravel transport rate, increasing the sand content should decrease the gravel transport rate by an amount proportional to its decreased proportion in the mixture. Because the proportional changes in gravel content are small (decreasing from 0.94 to

0.66 over the range of sediments) relative to the scale of the transport axis, one would expect that the gravel transport rates would fall within a single swath reflecting experimental variation. Instead, the gravel transport rates for the sandier beds fall consistently above those of the less sandy beds. Adding sand to the bulk mixture clearly increases the transport rate of the gravel portion of the load.

Transport rate plotted as a function of τ (Figures 4b and 4d) provides a cleaner separation of the transport trends for the different sediment mixtures. The trend between gravel transport rate and τ is nearly the same for J06 and J14 and increases consistently with increasing sand content such that at a constant τ the sandiest mixture (BOMC) has a transport trend 2 or more orders of magnitude above that for J06 and J14 (Figure 4d). The increase in q_g is largest between J14 and J27 (Figure 4d).

5. Comparison With Standard Scaling

As sand is added to a gravel mixture, the overall size distribution becomes finer. Because transport rate scales inversely with grain size, the increase in transport rate we observe with increasing f_s might be attributed to a reduction in the grain size of the mixture. Here we use a standard scaling of the relation between transport rate and grain size to evaluate whether the increases we observe in total transport rate and gravel transport rate might be predicted from the reduction in mixture grain size.

Total transport rate may be scaled with the overall mixture grain size, which can be represented using a characteristic grain size such as the median D_{50} . For unisize sediment this relation is directly embodied in the Shields number τ^* typically used to model transport rates

$$\tau^* = \frac{\tau}{(s-1)\rho g D_{50}}, \quad (1)$$

where s is the ratio of sediment density ρ_s to water density ρ , g is gravitational acceleration, and τ is shear stress. Transport rate is a nonlinear function of τ^* , which has led to the formulation of transport models in terms of $\tau^* - \tau^*_c$ or τ^*/τ^*_c , where τ^*_c is the critical value of τ^* defining the threshold of sediment transport [e.g., *Meyer-Peter and Müller, 1948; Yalin, 1977*]. If a single relation between dimensionless transport rate and τ^*/τ^*_c is found to hold for sediments of different grain size, size-dependent effects on transport are isolated to the variation of τ^*_c with grain size. For unisize sediment in the gravel size range, τ^*_c is approximately constant, indicating that τ_c increases, and τ^*/τ^*_c decreases, linearly with D . This scaling has also been observed to hold approximately for D_{50} of mixed-size sediments [Wilcock, 1993].

The critical shear stress for the total transport rate of the five mixtures can be estimated using the reference shear stress τ_r that produces a small dimensionless reference transport rate $W^* = 0.002$ [Parker et al., 1982; Wilcock, 1988] where

$$W^* = \frac{(s-1)gq_b}{u_*^3} \quad (2)$$

and $u_* = (\tau/\rho)^{0.5}$. W^* for the total transport rates are shown in Figure 5a, along with values of τ_{rt} used to scale τ in Figure 5b. The similarity collapse for the total transport rate is reasonably strong, indicating that most of the variation in transport rate from mixture to mixture is captured by τ_{rt} . If the increase in transport with increasing f_s were due solely to the reduction in D_{50} , we would expect τ_{r50}^* to remain relatively constant from mixture to mixture, or to decrease slightly, following the trace of the standard unisize Shields curve (Figure 5c). Instead, τ_{r50}^* decreases rapidly with decreasing D_{50} , indicating that increasing f_s increases total transport rate beyond that which may be attributed to grain size alone. Using D_{50} of the bulk size distribution to form τ_{r50}^* , values are close to typical unisize values (≈ 0.045) for the low sand mixtures J06 and J14 but decrease to very small values for the three sandier mixtures, with τ_{r50}^* as small as 20% of the unisize Shields values. Scaling the Shields number using surface grain size moderates this difference somewhat, with τ_{r50}^* taking typical surface-based values of ≈ 0.035 (a 23% reduction from standard Shields values) for the low sand mixtures and decreasing to 0.014 (a 62% reduction from Shields values) for the two sandiest mixtures.

When considering the transport of the gravel only, comparison of observed transport rates with conventional estimates requires accounting for the change in both relative and absolute grain size as sand content is increased. As D_{50} decreases, any gravel fraction (or the median D_g of all gravel fractions used here) becomes larger relative to D_{50} . The variation of fraction critical shear stress τ_{ci} with grain size is often approximated as

$$\tau_{ci} = \tau_{c50} \left(\frac{D_i}{D_{50}} \right)^b, \quad (3)$$

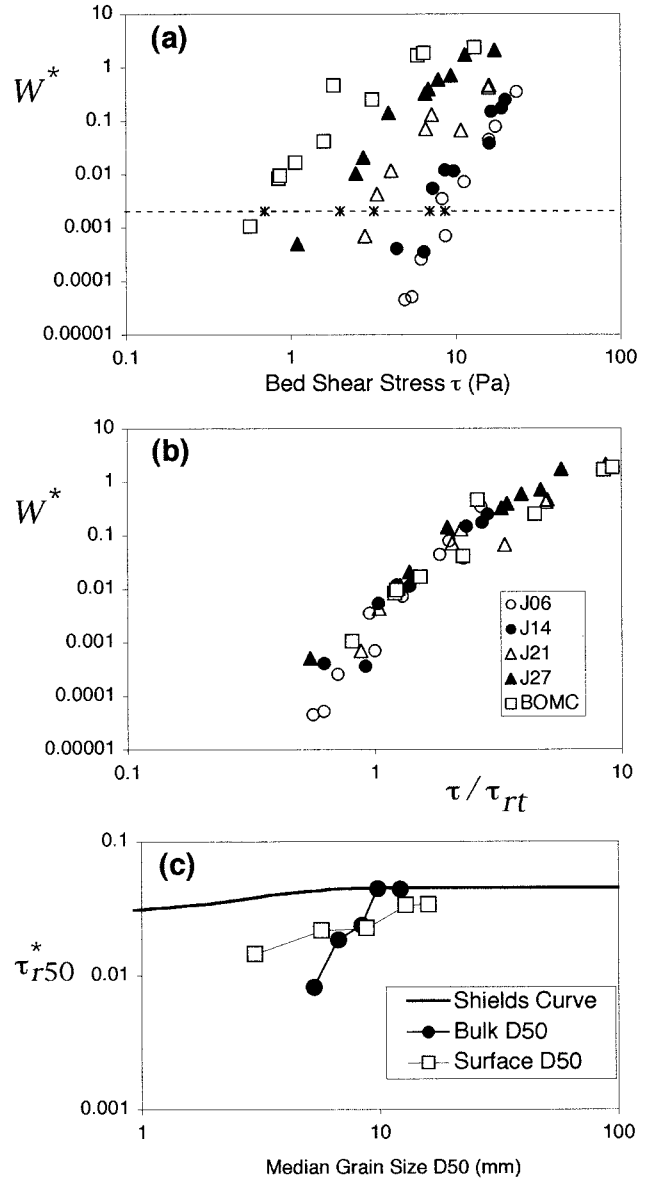


Figure 5. Analysis of total transport rate. (a) Dimensionless transport rate W^* as a function of bed shear stress, showing the reference value $W^* = 0.002$ and the values of reference shear stress τ_{rt} for each mixture. (b) W^* as a function of τ/τ_{rt} , using values of τ_{rt} indicated in Figure 5a. (c) Shields number τ_{r50}^* formed using τ_{rt} and D_{50} of either bulk or surface size distributions as a function of median grain size of bulk or surface size distributions. D_{50} increases consistently from the sandiest mixture (bed of many colors (BOMC)) to the least sandy mixture (J06).

where b typically takes a value between 0 and 0.3 [e.g., *Parker et al., 1982; Andrews and Parker, 1987; Wilcock, 1988, 1993*]. Expressed in terms of Shields number for the reference shear stress of gravel, this is

$$\tau_{rg}^* = \tau_{r50}^* \left(\frac{D_g}{D_{50}} \right)^{b-1}, \quad (4)$$

indicating that adding sand will change τ_{rg}^* in proportion to the change in τ_{r50}^* reduced by the change in relative grain size (D_g/D_{50}). Transport rates for the gravel (Figures 6a and 6b) collapse similarly to those for the total transport (Figures 5a

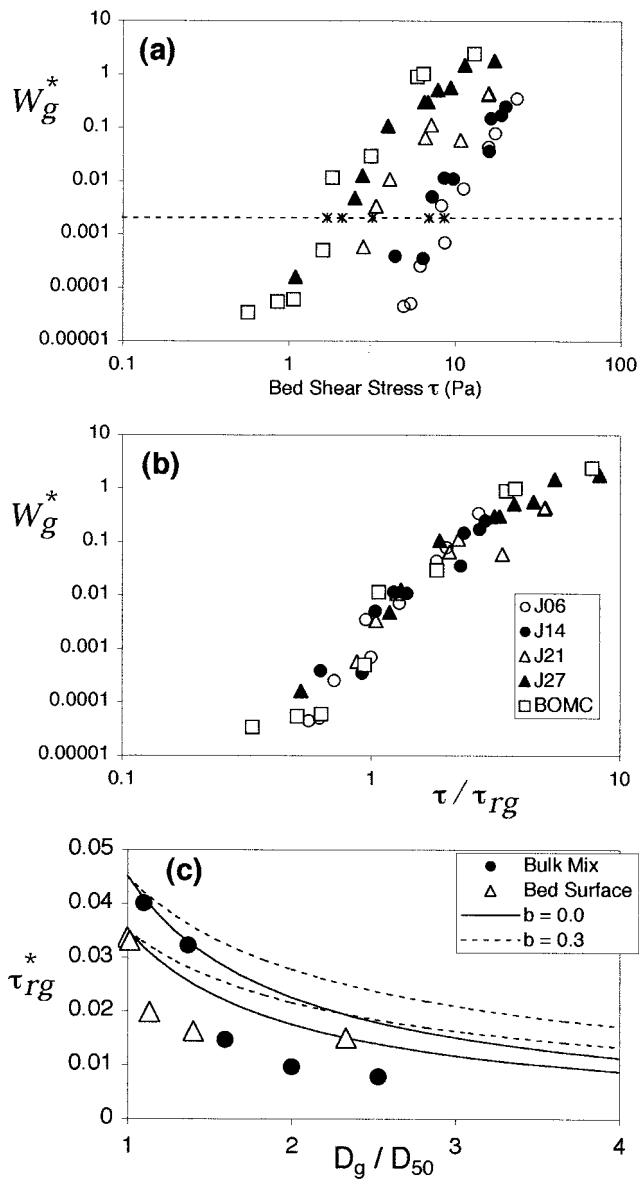


Figure 6. Analysis of gravel transport rate. (a) Dimensionless gravel transport rate W_g^* as a function of bed shear stress, showing the reference value $W_g^* = 0.002$ and the values of reference shear stress τ_{rg} for each mixture. (b) W_g^* as a function of τ/τ_{rg} , using values of τ_{rg} indicated in Figure 6a. (c) Shields number τ_{rg}^* formed using τ_{rg} and D_g of either bulk or surface size distributions as a function of relative grain size D_g/D_{50} based on either bulk or surface size distributions. D_g/D_{50} increases consistently from the least sandy mixture (J06) to the sandiest mixture (BOMC). Curves are equation (4) using τ_{r50}^* of 0.045 and 0.035.

and 6b), indicating that τ_{rg}^* captures most of the sand effect on gravel transport rates. Observed values of τ_{rg}^* are given in Figure 6c, along with estimates of τ_{rg}^* from (4) using $\tau_{r50}^* = 0.045$ (typical for subsurface grain size) and $\tau_{r50}^* = 0.035$ (typical for surface grain size) and $b = 0$ and $b = 0.3$, bracketing typical values of these parameters. For τ_{rg}^* formed using D_g of the bulk size distribution, observed values are similar to estimated values for the low sand mixtures J06 and J14 but drop well below the estimated values for the sandier mixtures. When the surface size distribution is used to form

τ_{rg}^* , observed values are again close to estimated values for the low sand mixtures but fall well below estimated values for the sandier mixtures, with the exception of BOMC. The reduction in observed τ_{rg}^* is similar to the reduction in τ_{r50}^* shown in Figure 5c.

The effect of adding sand on either the total transport rate or the gravel transport rate is evidently stronger than that which can be estimated based on the reduction in mixture grain size alone [Wilcock, 1998]. The increased mobility due to adding sand is captured in a reduction in the reference shear stress, which indicates that its effect on transport rate will be strongly nonlinear, increasing without bound as τ^* approaches τ_c^* in most standard transport formulas.

Standard scaling relations between transport rate and grain size do not adequately represent the effect of f_s on gravel transport rate, suggesting that current models of mixed-size transport may need to be revised. P. R. Wilcock and S. T. Kenworthy (A two-function model for the transport of sand/gravel mixtures, submitted to *Water Resources Research*, 2001) (hereinafter referred to as Wilcock and Kenworthy, submitted manuscript, 2001) develop the approach of Wilcock [1998] into a model for predicting the effect of f_s on gravel transport rates. By considering the sediment as a binary mix of two fractions, sand and gravel, the model can account for the effect of f_s on transport in a simple and direct manner.

6. Discussion

A variety of processes (e.g., logging, fire, land development, and reservoir flushing) can increase the supply of fine sediment to a gravel bed river. If this causes f_s of the river bed to increase, our results indicate that the transport capacity for both sand and gravel will increase, which can limit the magnitude of channel adjustment to the increased sediment supply and may also cause the river to evacuate the excess sediment in a shorter time than would be estimated from conventional models. Application of these results to the field requires a model that generalizes the experimental results given here, and further discussion is given by Wilcock and Kenworthy (submitted manuscript, 2001), who present such a model.

Application of our results to the field also requires specifying a size boundary between fine and coarse sediment. The threshold used here is 2 mm. Although this is the standard boundary between sand and gravel and represents an appropriate boundary in many field cases, it is essentially arbitrary. We expect that a larger boundary would be appropriate for some coarser sediments. For example, we have used a boundary of 8 mm on a coarse gravel/cobble river with a distinct fine mode in the sand and pea gravel range [Wilcock et al., 1996]. Further discussion of the choice of size boundary is given by Wilcock and Kenworthy (submitted manuscript, 2001), which interprets the effect on transport rate of fines content in terms of the relative proportion of matrix and framework grains.

7. Conclusions

Transport measurements using five sediments with different sand content indicate that total transport rate and gravel transport rate depend strongly on sand content. The effect of sand content on transport was isolated by using the same gravel population and varying only the proportion of sand from mixture to mixture. Flow depth was also held within a narrow range, and discharge was varied to produce a wide range of

transport rates with each sediment. For the same flow strength we observe that gravel transport rates increase by orders of magnitude as sand content is increased, despite the fact that the amount of gravel available for transport decreases as sand content increases. The increase in gravel transport rate is most rapid between the mixtures containing 14, 21, and 27% sand, which corresponds approximately to the transition from a framework-supported to a matrix-supported sediment bed.

These results support and extend earlier observations of an increase in gravel transport rate with increasing sand content. The present experiments use sediment with a wide range of sizes representative of many gravel bed streams and a sediment-recirculating arrangement that allows a direct correlation between bed composition and transport rate.

The bed surface composition was measured at the end of each run, providing a set of coupled flow/transport/bed surface observations for a wide range of transport rates with all five sediment mixtures. These data provide the opportunity to explore mixed-size transport models referenced to the bed surface, an essential component of a general model capable of predicting transient conditions. The bed surface grain size varies strongly with sand content but shows little or no coarsening with flow strength. This casts doubt on the idea that armor layers form at small flows and weaken or vanish with increasing flow and transport rate. As flow strength increases, the minor surface coarsening we observe may be attributed to the entrainment of an increasing proportion of coarse grains from the bed surface. This increases the opportunity for coarsening through kinematic sorting, the primary mechanism by which recirculating flume beds may armor.

The effect of sand content on transport rate is larger than would be predicted using standard scaling relations between transport rate and the reduction in grain size associated with increasing sand content. Models of mixed-size transport and of stream channel response to varying sediment inputs require revision to account for the influence of variable sand content. The effect of sand content on transport rate may be largely isolated to its effect on the critical shear stress for incipient motion. A model that includes the effect of sand content on sand and gravel incipient motion is proposed by Wilcock and Kenworthy (submitted manuscript, 2001).

Acknowledgments. This work was funded by the U.S. Department of Justice, Environment and Natural Resources Division. Conversations with Bill Emmett, Jack King, Gary Parker, Larry Schmidt, Peter Whiting, and Reds Wolman helped refine our analysis.

References

Andrews, E. D., and G. Parker, Formation of a coarse surface layer as the response to gravel mobility, in *Sediment Transport in Gravel-Bed Rivers*, edited by C. R. Thorne, J. C. Bathurst, and R. D. Hey, pp. 269–325, John Wiley, New York, 1987.

- Chiew, Y.-M., and G. Parker, Incipient sediment motion on non-horizontal slopes, *J. Hydraul. Res.*, 32(5), 649–660, 1994.
- Church, M. A., D. G. McLean, and J. F. Wolcott, River bed gravels: Sampling and analysis, in *Sediment Transport in Gravel-Bed Rivers*, edited by C. R. Thorne, J. C. Bathurst, and R. D. Hey, pp. 43–88, John Wiley, New York, 1987.
- Dietrich, W. E., J. W. Kirchner, H. Ikeda, and F. Iseya, Sediment supply and the development of the coarse surface layer in gravel-bedded rivers, *Nature*, 340, 215–217, 1989.
- Fernandez Luque, R., and R. Van Beek, Erosion and transport of bedload sediment, *J. Hydraul. Res.*, 14(2), 127–144, 1976.
- Ikeda, H., and F. Iseya, Experimental study of heterogeneous sediment transport, *Pap. 12*, Environ. Res. Cent., Univ. of Tsukuba, Tsukuba, Japan, 1988.
- Jackson, W. L., and R. L. Beschta, Influences of increased sand delivery on the morphology of sand and gravel channels, *Water Resour. Bull.*, 20(4), 527–533, 1984.
- Kellerhals, R., and D. I. Bray, Sampling procedures for coarse alluvial sediments, *J. Hydraul. Div., Am. Soc. Civ. Eng.*, 97(HY8), 1165–1180, 1971.
- Meyer-Peter, E., and R. Müller, Formulation for bed load transport, paper presented at 2nd Congress, Int. Assoc. of Hydraul. Res., Stockholm, 1948.
- Parker, G., Surface-based bedload transport relation for gravel rivers, *J. Hydraul. Res.*, 28(4), 417–436, 1990.
- Parker, G., and P. C. Klingeman, On why gravel bed streams are paved, *Water Resour. Res.*, 18(5), 1409–1423, 1982.
- Parker, G., and P. R. Wilcock, Sediment feed and recirculating flumes: A fundamental difference, *J. Hydraul. Eng.*, 119(11), 1192–1204, 1993.
- Parker, G., P. C. Klingeman, and D. L. McLean, Bedload and size distribution in paved gravel-bed streams, *J. Hydraul. Div. Am. Soc. Civ. Eng.*, 108(HY4), 544–571, 1982.
- Vanoni, V. A., and N. H. Brooks, Laboratory studies of the roughness and suspended load of alluvial streams, *Sediment. Lab. Rep. E68*, Calif. Inst. of Technol., Pasadena, 1957.
- Wilcock, P. R., Methods for estimating the critical shear stress of individual fractions in mixed-sized sediment, *Water Resour. Res.*, 24(7), 1127–1135, 1988.
- Wilcock, P. R., The critical shear stress of natural sediments, *J. Hydraul. Eng.*, 119(4), 491–505, 1993.
- Wilcock, P. R., Two-fraction model of initial sediment motion in gravel-bed rivers, *Science*, 280, 410–412, 1998.
- Wilcock, P. R., The flow, the bed, and the transport: Interaction in flume and field, in *Proceedings of the Fifth Gravel-Bed Rivers Workshop*, edited by P. Mosley, pp. 183–219, N. Z. Hydrol. Soc., Wellington, 2001.
- Wilcock, P. R., and B. W. McArdell, Surface-based fractional transport rates: Mobilization thresholds and partial transport of a sand-gravel sediment, *Water Resour. Res.*, 29(4), 1297–1312, 1993.
- Wilcock, P. R., and B. W. McArdell, Partial transport of a sand-gravel sediment, *Water Resour. Res.*, 33(1), 233–245, 1997.
- Wilcock, P. R., G. M. Kondolf, W. V. G. Matthews, and A. F. Barta, Specification of sediment maintenance flows for a large gravel-bed river, *Water Resour. Res.*, 32(9), 2911–2921, 1996.
- Yalin, M. S., *Mechanics of Sediment Transport*, Pergamon, New York, 1977.

J. C. Crowe, S. T. Kenworthy, and P. R. Wilcock, Department of Geography and Environmental Engineering, Johns Hopkins University, Baltimore, MD 21218, USA. (wilcock@jhu.edu)

(Received May 10, 2001; revised August 28, 2001; accepted August 30, 2001.)